RESEARCH PAPER

Investigating the Effect of Wire Electrical Discharge Machining Factors for Ductile Cast Iron (ASTM A536)

Marwa M. El-Mahalawy[1], M. SAMUEL[2], N. Fouda[3] & Sara A. El-Bahloul*[4]

ABSTRACT
Wire Electrical Discharge Machining (WEDM) is a non-traditional thermal machining process used to manufacture irregularly profiled parts. Machining of ductile cast iron (ASTM A536) under several machining factors, which affect the WEDM process, is presented. The considered machining factors are pulse on time (T_{on}), pulse off (T_{off}), peak current (Ip), voltage (V), and wire speed (S). To optimize the machining factors, their setting is performed via an experimental design using the Taguchi method. The optimization objective is to achieve maximum Material Removal Rate (MRR) and minimum Surface Roughness (SR). Additionally, the analysis of variance (ANOVA) is used to identify the most significant factor. Also, a regression analysis is carried out to forecast the MRR and SR dependent on defined machining factors. Depending on consequences, the best regulation factors for reaching the maximum MRR are T_{on} = 32 µs, T_{off} = 8 µs, Ip = 4 A, S = 40 mm/min. and V = 70 volt. Whereas, the optimal control factors that achieve the minimum SR is T_{on} = 8 µs, T_{off} = 8 µs, Ip = 2 A, S = 20 mm/min, and V= 30 volt. It is hypothesized that the perfect combination of control factors that achieves minimum SR and maximum MRR is T_{on} = 8 µs, T_{off} = 8 µs, Ip=5 A, S=50 mm/min. The microstructure of the machined surface in the optimal machining conditions shows a very narrow recast layer at the top of the machined surface.

KEYWORDS: *Wire electrical discharge machining; Material removal rate; Surface roughness; Taguchi; Analysis of variance; Regression analysis.*

1. Introduction

Non-Traditional Machining Processes (NTMPs) use different energies in their direct form instead of tools. NTMPs are better than traditional processes as they can machine a wide range of metallic and non-metallic materials regardless of their hardness or strength as there is no physical contact between the workpiece and the tool. Besides, NTMP can produce complex and intricate shapes with high accuracy and surface quality [1]. WEDM is thermal non-traditional machining in which the material is removed from the workpiece due to the spark that happens between the workpiece and the wire in the presence of a thin film of dielectric fluid. WEDM is widely used in the aerospace, automotive, and medical industries, with very complicated geometries [2, 3].

Ductile cast iron is essentially a class of cast iron which is distinguished in the structure by spherical graphite nodules. Ductile cast iron (ASTM A536) is a nodular iron with a predominantly ferritic microstructure and similar mechanical properties of low alloy steels. It has outstanding properties such as good machinability and castability, enhanced strength and toughness, strengthened wear resistance, and low casting performance. These properties allow it to be used effectively in a broad range of industrial applications including piping, vehicle parts, wheels, gearboxes, pump housings, wind power system frames, and many more [4].

Several studies were carried out on the optimization of the WEDM process. B. Mathew et al. employed Taguchi grey relation analysis to determine the optimum machining parameters while machining AISI304. The results indicated that the pulse on time was the most important parameter because when it increased the material removal rate decreased and the surface roughness

* Corresponding author: *Sara A. El-Bahloul*
sara_elbahloul@mans.edu.eg

1. *Higher Future Institute of Engineering & Technology, Mansoura, Egypt.*
2. *Production & Mechanical Design Engineering Department, Faculty of Engineering, Mansoura University, Egypt.*
3. *Production & Mechanical Design Engineering Department, Faculty of Engineering, Mansoura University, Egypt.*
4. *Production & Mechanical Design Engineering Department, Faculty of Engineering, Mansoura University, Egypt.*

increased [5]. D. A. Raj and T. Senthilvelan optimized the cutting conditions of WEDM for better surface roughness and material removal rate of D2 tool steel. Box-Benkhen approach was used as the experimental strategy, while the multiple parameter optimization was performed using desirability functions. The results revealed that the pulse on time and the pulse off time were the most effective parameters that influenced the surface roughness, whereas the pulse off time had a major influence on the material removal rate [6]. P. Kumar Karsh used Taguchi and ANOVA methods to optimize the process parameters for achieving better surface roughness of Inconel 625. The result shows that the pulse current is an insignificant parameter and the surface roughness increased with increasing the pulse on time and decreasing the pulse of time [7]. V. R. Surya et al. predicted machining characteristics of Al7075-TiB2 using Taguchi L27 orthogonal array and Artificial Neural Network. The results indicated that 70 % of the training sets correlated well with the measured values [8]. R. Sen et al. established neural network models to predict cutting speed, surface roughness, and wire consumption while cutting steel 300. The result showed that the used fuzzy logic methodology presented a better alternative to parametric optimization [9]. A. Abioye et al. established an artificial neural network model coupled with Taguchi to predict maximum MRR and minimum SR values for machining AISI 1045 steel. The results indicated that Ton was the most significantly affecting parameter followed by Toff [10]. S. A. El-Bahloul used statistical methods coupled with artificial intelligence techniques and soft computing to optimize the WEDM of AISI304

stainless steel. The results investigated that fine surface roughness was achieved by decreasing the pulse current and pulse on time as well as increasing pulse of time despite achieving a lower material removal rate [11]. P. Satishkumar et al. studied MRR and SR based on the process parameters of WEDM based on Taguchi and regression equations. The result indicated that Ton was the most significant parameter followed by Toff and wire tension [12]. D. Palanisamy et al. investigated the method of texture fabrication and performance analysis of machinability for a textured and conventional Tungsten Carbide tool inserts. Taguchi's experimental design was used to optimize the cutting force and SR. The results indicated that machining with textured inserts achieved lower cutting forces and SR than conventional insert [13].

From previous work, no research has investigated the effect of different machining factors while cutting ductile cast iron despite its great importance and applications. Table 1 illustrates a comprehensive research gap analysis that compares the literature survey and the proposed work. This work aims to optimize the most important machining factors such as Ton, Toff, Ip, V, and S while cutting ductile cast iron (ASTM A536) to achieve the maximum MRR and the minimum SR. The optimization approach used in this work is based on the Taguchi method coupled with ANOVA and regression analysis. Besides, the response optimizer is used to obtain the optimum combination of control factors that achieves the ideal of both the SR and the MRR. The statistical analysis, which is needed to be accomplished during this work, is performed with the help of Minitab software.

Tab. 1. Comparison between previous studies and the proposed study

Authors	year	Aim	Workpiece Material	Method	Input parameter	Output parameter
B. Mathew, et al.,	2014	Optimization	AISI304	Taguchi (L27)	T_{on}, T_{off}, V, wire feed, wire tension, and dielectric pressure	SR, MRR, and dimension deviation
D. A. Raj and T. Senthilvelan	2015	Optimization	Ti6Al4V alloy	BoxBenkhen approach	T_{on}, T_{off}, and power feed	SR and MRR
P. Kumar Karsh	2016	Optimization	Inconel 625	Taguchi (L9) + ANOVA	T_{on}, T_{off}, and I_p	SR
V. R. Surya, et al.,	2017	Prediction	Al7075	Taguchi (L27) + Artificial Neural Network	T_{on}, T_{off}, I_p, and S	SR, MRR, and dimension error
R. Sen, et al.,	2017	Prediction	Steel 300	Neural	T_{on}, T_{off}, V, I_p,	Cutting

					network	and wire tension	speed, SR, and wire consumption
A. Abioye, et al.,	2018	Prediction	AISI 1045		Taguchi (L27)+ ANOVA+ Artificial neural network	T_{on}, T_{off}, and V	MRR and SR
S. A. El-Bahloul	2020	Optimization and Prediction	AISI 304 stainless steel		Response surface methodology + Artificial neural network	T_{on}, T_{off}, and I_p	MRR and SR
P. Satishkumar, et al.,	2020	Optimization	OFHC copper		Taguchi (L9)	T_{on}, T_{off}, and wire feed	MRR and SR
D. Palanisamy, et al.,	2020	Studying fabrication and machinability performance	17–4 PH Stainless Steel		Taguchi-Grey Relational Approach	Speed, Feed, and tool insert type	SR and cutting force
M.M. El-Mahalawy	2021	Optimization and Prediction	ASTM536		Taguchi L32 + ANOVA + Regression analysis + Optimization tool	T_{on}, T_{off}, V, I_p, and S	SR and MRR

2. Experimental Setup

Taguchi approach is used to construct the experimental design, in order to reduce the experimental trials [14]-[15]. In order to attain the optimal machining factors combination that achieves minimum SR and maximum MRR. Five important control factors are considered. Table 2 shows the control factors with their levels. Based on pilot tests, each factor level value is selected. Accordingly, an orthogonal array (L32) with missed levels is employed for the experimental work. Table 3 displays the experimental design, which is performed with the aid of Minitab software.

Tab. 2. The control factors and their levels

Factor Name	Factor symbol	unit	Levels			
			1	2	3	4
Pulse on time	T_{on}	μs	8	16	32	64
Pulse off time	T_{off}	μs	8	10	12	14
Wire speed	S	mm/min	20	30	40	50
Peak current	Ip	Ampere	2	3	4	5
Voltage	V	volt	30	80	-	-

Tab. 3. L32 experimental design matrix with the control and response factors

Run No.	Control factor					Response factor			
						Experimental		Predicted	
	V	T_{on}	T_{off}	Ip	S	MRR mm^3/min	SR μmRa	MRR mm^3/min	SR μmRa
1	30	8	8	2	20	4.561	2.263	4.727	2.901
2	30	8	10	3	30	5.456	3.060	5.957	3.011
3	30	8	12	4	40	6.170	2.826	7.187	3.120
4	30	8	14	5	50	6.660	2.986	8.416	3.230

5	30	16	8	2	30	4.990	2.720	5.383	2.996
6	30	16	10	3	20	6.170	3.460	5.553	3.228
7	30	16	12	4	50	7.416	3.643	7.843	3.215
8	30	16	14	5	40	9.522	3.656	8.013	3.447
9	30	32	8	3	40	9.253	3.383	7.756	3.695
10	30	32	10	2	50	5.607	3.616	5.806	2.909
11	30	32	12	5	20	9.096	3.983	8.096	4.158
12	30	32	14	4	30	6.942	3.500	6.146	3.372
13	30	64	8	3	50	8.950	4.450	8.792	4.258
14	30	64	10	2	40	5.080	3.886	5.782	3.594
15	30	64	12	5	30	9.149	4.793	9.131	4.721
16	30	64	14	4	20	5.655	3.706	6.121	4.057
17	80	8	8	5	20	8.240	7.870	10.83	4.819
18	80	8	10	4	30	8.890	3.250	8.883	4.032
19	80	8	12	3	40	7.050	2.583	6.933	3.246
20	80	8	14	2	50	4.530	2.516	4.983	2.459
21	80	16	8	5	30	11.923	3.730	11.490	4.914
22	80	16	10	4	20	9.087	3.550	8.480	4.249
23	80	16	12	3	50	7.588	3.586	7.59	3.341
24	80	16	14	2	40	5.162	3.236	4.579	2.678
25	80	32	8	4	40	12.453	4.983	10.683	4.717
26	80	32	10	5	50	12.350	4.480	11.913	4.826
27	80	32	12	2	20	4.760	2.883	4.662	3.388
28	80	32	14	3	30	7.170	3.566	5.892	3.497
29	80	64	8	4	50	11.880	5.023	11.718	5.280
30	80	64	10	5	40	10.940	5.146	11.888	5.511
31	80	64	12	2	30	4.580	4.196	5.698	3.951
32	80	64	14	3	20	5.460	4.510	5.868	4.182

The processing of the experiments is performed on JIANGSU SANXING electric spark wire cutting machine (Model DK77-50AZ). Ductile cast iron (ASTM A536) is used as the workpiece material of dimensions 110×100×11 mm. Table 4 shows the chemical composition of the implemented material. The cutting profile represents a cuboid having a cross-sectional area of 10×10 mm and a thickness of 11 mm. A molybdenum wire of 0.18 mm diameter is applied as a tool. Deionized water is applied in the gap between the tool and the workpiece. Figure 1 demonstrates the workpiece cutting while performing the experimental work.

Tab. 4. Chemical composition of ASTM A536

	C	Mn	Si	S	P
Chemical composition wt%	3.5-3.9%	0.15-0.35%	2.25-2.75%	0.01-0.025%	0.05% maximum

Fig.1. processing of the workpiece during performing the experimental work

The considered process output to identify the optimal process parameters are the MRR and SR. The MRR is the amount of material removed per time unit, so it is a direct indicator of the cutting efficiency and the process profit. Besides, good surface roughness means high machining quality [16].

The SR is measured five times using MITUTOYO SURFTEST SJ 201P. The measuring instrument traces the surface of the machined workpiece and calculates the Ra based on the roughness standards [17]. The SR average for each experiment is reported in Table 3.

The MRR is calculated using Equations (1)-(3) [18].

$$MRR = Kw * Vc * Mt \qquad (1)$$
$$Kw = wd + (2 \times offset) \qquad (2)$$
$$Vc = machining\ length\ /\ machining\ time \qquad (3)$$

where Kw is the kerf width, Vc is the cutting velocity, Mt is the workpiece thickness, and wd is the wire diameter.

3. Result and Discussion
3.1. Response graphs

The response graphs are used to understand the influence of each control factor level on the response factors [19]. Figure 2 shows the response graphs for the MRR and the SR. It is clear that Ip is the major factor that affects the MRR and the SR. Figure 2 (a) illustrates the response graph for the MRR. When Ip and V increase, the MRR increases, while by increasing T_{off}, the MRR decreases. When T_{on} increases, the MRR increases until it reaches 64 μ sec; then, it begins to decrease due to the unstable discharge compared to the workpiece thickness. When S increases, the MRR increases until it reaches 50 mm/min; then, it slightly decreases.

Figure 2 (b) displays the response graph for the SR. It is clear that by increasing V, T_{on}, Ip and decreasing T_{off}, the SR increases. By decreasing S, the SR decreases until it reaches 30 mm/min; then, it begins to increase due to the increase in the contact time between the wire and the workpiece, leading to a rougher surface.
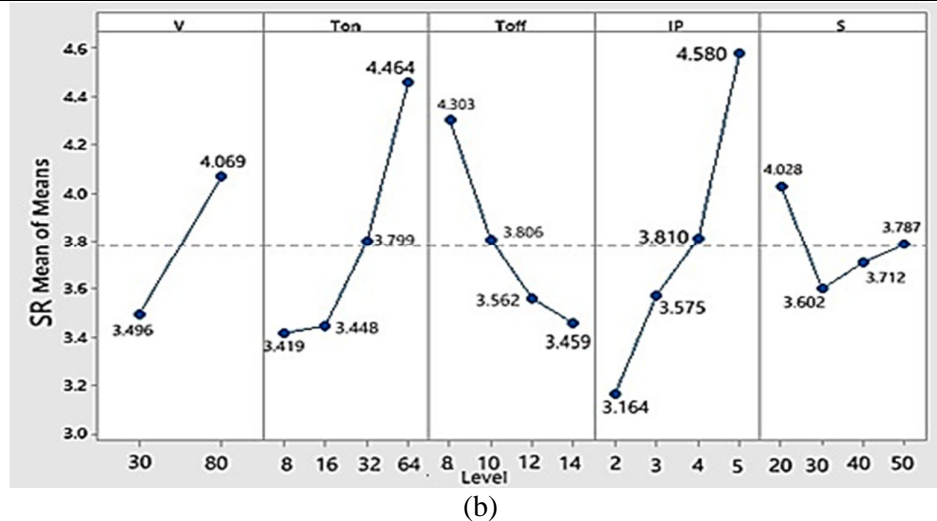

(a)

(b)
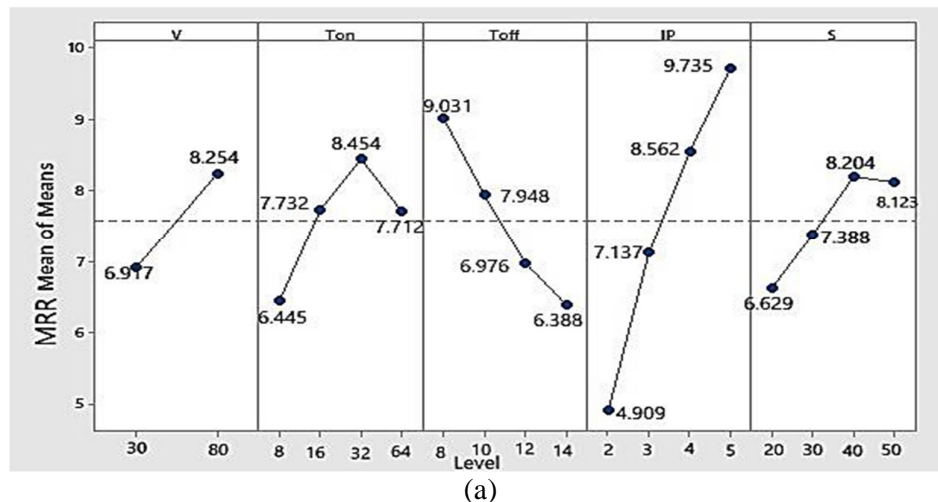
Fig. 2. Response graphs for (a) MRR and (b) SR

3.2. ANOVA

The Taguchi method cannot judge and calculate the impact of individual parameters on the whole process, while ANOVA can accurately determine the percentage contribution of individual parameters [20]-[21]. It is conducted to explain the statistical analysis effect of the control factors on the response factors. Table 5 represents the ANOVA for the MRR and the SR. It can be seen that all the control factors have a significant effect on the MRR as the P-value is less than

0.05. Additionally, it is clear that Ip is a major influencing factor as it achieves the highest contributions percentage (49.7 %), followed by V, Toff, Ton, and S. For the SR, it is obvious that Ip is the major influencing factor, contributing by 32.3%. The factors Ton, Toff, S, and V are not significant as their P-value is higher than 0.05. Figure 3 illustrates the contribution percentage of ANOVA for the MRR and SR.

Tab. 5. ANOVA for MRR and SR

MRR						
Source	Degree of freedom	Adjusted sum of squares	Adjusted mean squares	F-value	P-value	Contribution %
V	1	14.293	14.2925	27.14	0.000	20.57
T_{on}	3	16.745	5.5817	10.60	0.000	8.03
T_{off}	3	32.220	10.7399	20.40	0.000	15.46
Ip	3	103.514	34.5045	65.53	0.000	49.7
S	3	13.004	4.3348	8.23	0.001	6.24
Error	18	9.478	0.5265			
Total	31	189.253				100
SR						
Source	Degree of freedom	Adjusted sum of squares	Adjusted mean squares	F-value	P-value	Contribution %
V	1	2.6318	2.6318	3.44	0.080	30.1
T_{on}	3	5.6678	1.8893	2.47	0.095	21.6
T_{off}	3	3.3946	1.1315	1.48	0.254	12.95
Ip	3	8.5012	2.8337	3.70	0.031	32.37
S	3	0.7832	0.2611	0.34	0.796	2.98
Error	18	13.7705	0.7650			
Total	31	34.7491				100

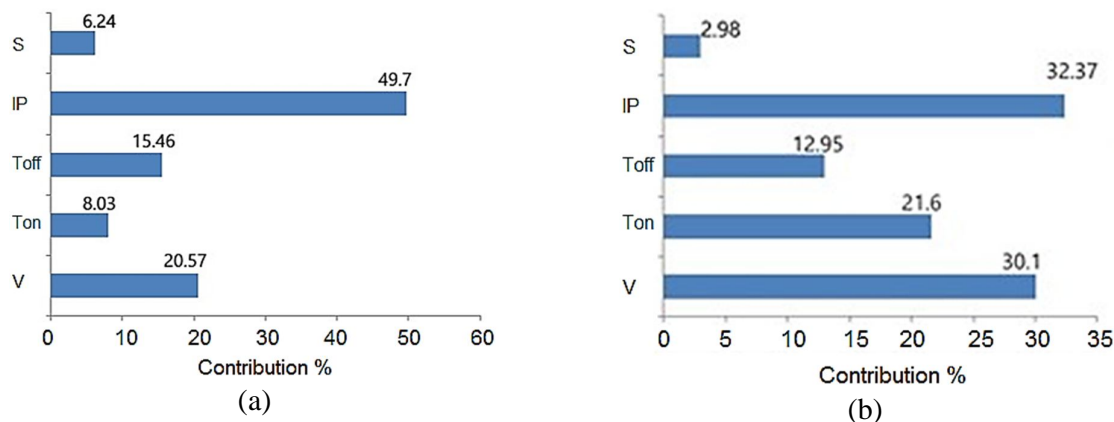(a)   (b)

Fig. 3. The contributions percent results of ANOVA for (a) MRR and (b) SR

3.3. Regression analysis

Regression equations are helpful in predicting the process output parameter instead of doing the experimental work at other levels than those on the matrix. It is used to estimate the relationship between the control and response factors for prediction and forecasting [22]. Equations (4) and (5) are the generated regression equations to predict the MRR and SR, respectively, at any control factor's value.

$$MRR=3.12+0.02673V+0.0158T_{on}-0.4451T_{off}+1.59Ip+0.053S \quad (4)$$

$$SR=2.737+0.01147V+0.0195T_{on}-0.1387T_{off}+0.448Ip-0.0061S \quad (5)$$

Table 2 shows the predicted MRR and SR values that are calculated using the regression equations. Figure 4 illustrates a comparison between the experimental and predicted results for the MRR and the SR. It is obvious that there is no large significant difference between the experimental and predicted values.
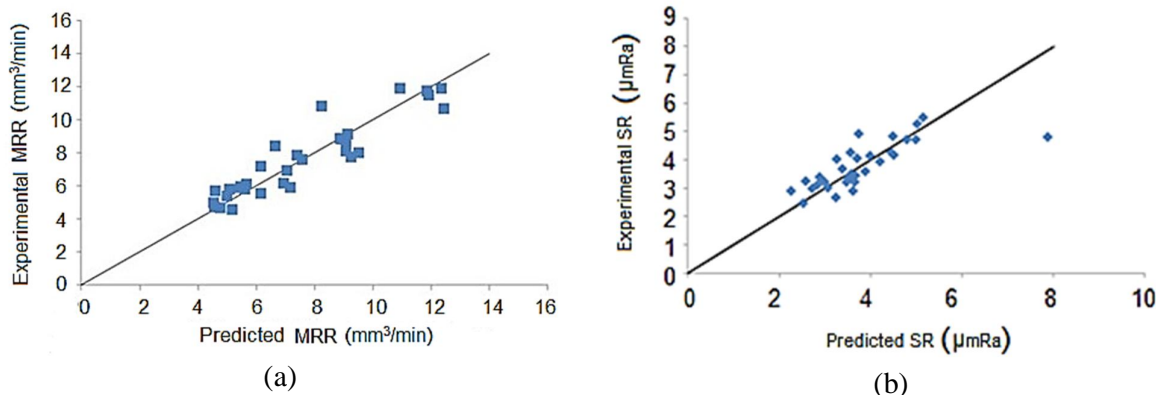

(a)   (b)

Fig. 4. Comparisons between the experimental and predicted values of (a) MRR and (b) SR

3.4. Optimization considering both the MRR and SR

A Minitab response optimizer tool is applied to reveal how various experimental settings change the expected responses for a stored model [23]. It is used to get the optimal control factors for optimizing both the MRR and the SR together as

shown in Fig. 5. The optimal control factors combination that achieves better SR and MRR together is T_{on} = 8 μs, T_{off} = 8 μs, Ip = 5 A, S = 50 mm/min, and V = 80 volt. The resultant predicted MRR and SR based on the regression equations (4) and (5) are 12.4219 and 4.3672 respectively as displayed in Fig. 5.
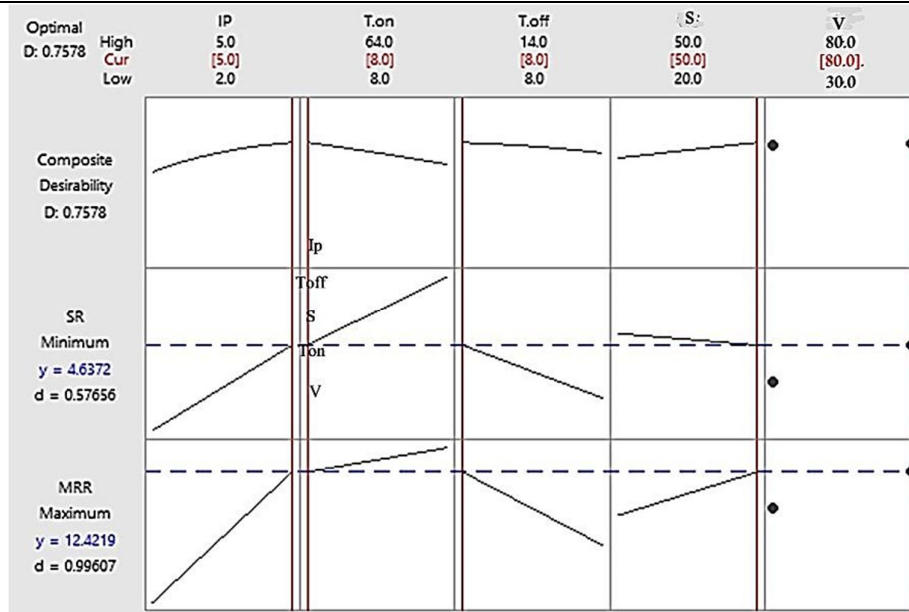
Fig. 5. Optimal control factors for optimizing both the MRR and SR together

A confirmation experiment is conducted based on the combination of optimal control factors that achieve better SR and MRR together. Table 6 shows the resulting experimental and predicted MRR and SR values in the optimal machining condition. It is obvious that an improvement of SR is achieved with a decrease in the MRR. Figure 6 shows the microstructure of the machined surface in optimal machining conditions. A very narrow recast layer can be seen at the top of the machined surface. Therefore, this study helps the industry achieve higher MRR, leading to shorter machining time span, which in effect decreases the net cost of the product. Also, the lower SR often leads to lower finishing requirements after machining.

Tab. 6. The resulting experimental and predicted MRR and SR values in optimal conditions

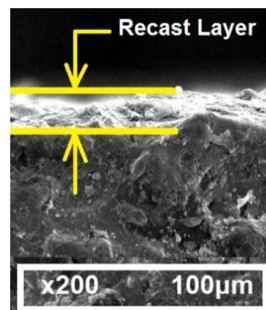| Responses	Experimental	Prediction
MRR (mm^3/min)	10.897	12.422
SR (μmRa)	3.13	4.637

Fig. 6. The machined surface microstructure

4. Conclusions

An optimization approach was implemented by applying the Taguchi technique, which is coupled with the ANOVA and the regression analysis, in order to achieve the maximum MRR and minimum SR with WEDM of ductile cast iron (ASTM A536). Taguchi method was applied to perform the experimental design based on the selected control factors such as T_{on}, T_{off}, Ip, V, and S. The response graph was used to reveal the influence of each control factor level on the response factors. ANOVA technique was employed to determine the most significant factor affecting the machining performance. Regression analysis was conducted to estimate the relationship between the control and response

factors for [prediction](#) and [forecasting.](#) The response optimizer was utilized to determine the optimal combination of control factors that optimize both the SR and the MRR together. It can be concluded that the IP is the a influencing factor that has a direct effect on both MRR and SR. The higher the Ip and the V and the lower of T_{off}, the higher the resulting values of MRR and SR. The optimal control factor combination that achieves the minimum SR is T_{on}=8 µs, T_{off}=8 µs, IP =2 A, S =20 mm/min, and V= 30 volt. The optimal control factors that achieve the maximum MRR are T_{on}=32µs, T_{off}=8 µs, Ip=4 A, S= 40 mm/min. The combination of optimal control factors that achieve better SR and MRR together include T_{on} = 8 µs, T_{off} = 8 µs, Ip = 5 A, S = 50 mm/min, and V = 80 volt. The microstructure of the machined surface in optimal machining conditions shows a very narrow recast layer at the top of the machined surface. This research helps the industry achieve higher MRR, thus achieving a shorter machining time span which in effect decreases the net cost of the product. Also, the lower SR often leads to less finishing requirements after machining. This work needs future studies for performing a computer aided process optimization system of WEDM with the help of finite element modeling.

References

[1] H. Y. and H. El-Hofy, *non-traditional and advanced machining technologies*, Secend. (2021).

[2] U. A. Dabade and S. S. Karidkar, "Analysis of Response Variables in WEDM of Inconel 718 Using Taguchi Technique," *Procedia CIRP*, Vol. 41, (2016), pp. 886-891.

[3] S. Datta and S. Mahapatra, "Modeling, simulation and parametric optimization of wire EDM process using response surface methodology coupled with grey-Taguchi technique," *Int. J. Eng. Sci. Technol.*, Vol. 2, No. 5, (2010), pp. 162-183.

[4] N. Fatahalla, S. Bahi, and O. Hussein, "Metallurgical parameters, mechanical properties and machinability of ductile cast iron," *J. Mater. Sci.*, Vol. 31, No. 21, (1996), pp. 5765-5772.

[5] B. Mathew, Benkim, and J. Babu, "Multiple Process Parameter Optimization of WEDM on AISI304 Using Taguchi Grey Relational Analysis," *Procedia Mater. Sci.*, Vol. 5, (2014), pp. 1613-1622.

[6] D. A. Raj and T. Senthilvelan, "Empirical Modelling and Optimization of Process Parameters of machining Titanium alloy by Wire-EDM using RSM," *Mater. Today Proc.*, Vol. 2, No. 4-5, (2015), pp. 1682-1690.

[7] P. Kumar Karsh, "Optimization of process parameters for surface roughness of Inconel 625 in Wire EDM by using Taguchi method," *IOSR J. Mech. Civ. Eng.*, Vol. 03, No. 03, (2016), pp. 58-63.

[8] V. R. Surya, K. M. V. Kumar, R. Keshavamurthy, G. Ugrasen, and H. V Ravindra, "ScienceDirect Prediction of Machining Characteristics using Artificial Neural Network in Wire EDM of Al7075 based In-situ Composite," *Mater. Today Proc.*, Vol. 4, No. 2, (2017), pp. 203-212.

[9] R. Sen, B. Choudhuri, J. D. Barma, and P. Chakraborti, "Optimization of wire EDM parameters using teaching learning based algorithm during machining of maraging steel 300," *Mater. Today Proc.*, Vol. 5, No. 2, (2018), pp. 7541-7551.

[10] A. A. A. Alduroobi, A. M. Ubaid, M. A. Tawfiq, and R. R. Elias, "Wire EDM process optimization for machining AISI 1045 steel by use of Taguchi method , artificial neural network and analysis of variances," *Int. J. Syst. Assur. Eng. Manag.*, Vol. 11, No. 6, (2020), pp. 1314-1338.

[11] S. A. El-Bahloul, "Optimization of wire electrical discharge machining using statistical methods coupled with artificial intelligence techniques and soft

computing," *SN Appl. Sci.*, Vol. 2, No. 1, (2020), pp. 1-8.

[12] P. Satishkumar, C. S. Murthi, and R. Meenakshi, "Materials Today : Proceedings Optimization of machining parameters in wire EDM of OFHC copper using Taguchi analysis," *Mater. Today Proc.*, No. xxxx, (2020).

[13] D. Palanisamy, N. Manikandan, R. Ramesh, M. Kathirvelan, and D. Arulkirubakaran, "Materials Today : Proceedings Machinability Analysis and Optimization of Wire-EDM Textured Conventional Tungsten Carbide Inserts in Machining of 17 – 4 PH Stainless Steel," *Mater. Today Proc.*, No. xxxx, (2020).

[14] M. R. Phate, S. B. Toney, and V. R. Phate, "Optimization of Performance Parameters for OHNS Die Steel using," *Int. J. Ind. Eng. Prod. Res.*, Vol. 30, No. 1, (2019), pp. 11-23.

[15] J. Antony, "Teaching the Taguchi method to industrial engineers," Vol. 50, No. 4, (2001), pp. 141-149.

[16] L. Polytechnic, "Surface Roughness-," vol. 2, no. September, (1981), pp. 260-265.

[17] A. Joshi and P. Kothiyal, "Investigating Effect of Machining Parameters of CNC Milling on Surface Finish by Taguchi Method," No. January 2012, (2019).

[18] J. G. R and A. N. Chapgaon, "Effect and Optimization of Process Parameters using Taguchi Method in WEDM for AISI M42 HSS Material," Vol. 6, No. 2, (2017), pp. 2329-2335.

[19] S. A. El-Bahloul and R. Mostafa, "Experimental and Statistical Optimization Of Wire- EDM For Hipped (HIP) Udimet700," *Int. J. Mech. Mechatronics Eng. IJMME-IJENS*, Vol. 21, No. 01, (2021).

[20] R. A. Armstrong, S. V Slade, and F. Eperjesi, "Statistical Review An introduction to analysis of variance (ANOVA) with special reference to data from clinical experiments in optometry," Vol. 20, No. 3, (2000).

[21] M. Phate, S. Toney, and V. Phate, "Investigation on the impact of silicon carbide and process parameters on Wire Cut-EDM of Al/SiCp MMC," *Int. J. Ind. Eng. Prod. Res.*, Vol. 31, No. 2, (2020), pp. 177-187.

[22] S. Tonidandel and J. M. Lebreton, "Relative Importance Analysis : A Useful Supplement to Regression Analysis," (2011), pp. 1-9.

[23] G. Koronis, A. Silva, and S. Foong, "Predicting the Flexural Performance of Woven Flax Reinforced Epoxy Composites Using Design of Experiments," *Mater. Today Commun.*, (2017).